Pergamon

Available online at www.sciencedirect.com
SCIENCE DIRECT®

Cement and Concrete Research 33 (2003) 1093–1101

CEMENT AND CONCRETE RESEARCH

Comparison of guarded and unguarded linear polarization CCD devices with weight loss measurements

Youping Liu, Richard E. Weyers*

Department of Civil and Environmental Engineering, Virginia Polytechnic Institute and State University, Blacksburg, VA 24061-0105, USA

Received 2 May 1999; accepted 9 January 2003

Abstract

Two types of linear polarization devices may be used to measure the corrosion current density (CCD) to assess the degree of active corrosion in concrete structures. The devices, with and without a guard electrode, provide significantly different CCD values for the same conditions. The 5-year study reported herein presents a comparison of the two devices over a range of CCD values from passive to highly active corrosion conditions for outdoor exposure slabs. The results demonstrate that both devices are able to qualitatively rank the instantaneous corrosion conditions in structures. The guarded electrode device measurements were less quantitatively precise than the unguarded electrode device. The guarded electrode device underestimated the amount of metal loss by a factor of 4–6. The unguarded electrode device overestimate the metal loss by a factor of about 1.5 when compared to weight loss measurements and adjusted for concrete temperature and resistance.

Keywords: Corrosion; Electrochemical properties; Chloride; Concrete; Linear polarization

1. Introduction

Corrosion of steel in reinforced concrete structures is generally considered a electrochemical process. Corrosion current density (CCD) is one of the key parameters for quantitatively predicting the corrosion service life of reinforced concrete structures and the need of repair or rehabilitation [1–3]. Because of the complex electrolytic characteristics of steel in concrete, it is difficult to develop accurate corrosion-monitoring devices for reinforced concrete structures. However, linear polarization techniques as the unguarded counter-electrode (UnCE) and the guarded counter electrode (GCE) have been used for measuring the CCD of steel in concrete structures. The measured CCD by linear polarization methods only provides an instantaneous corrosion response to the concrete temperature and moisture conditions at the measurement moment. Factors which significantly influence the corrosion process and thus the measured CCD need to be further investigated in order to adjust the instantaneous measured value to a value for predicting service-life performance. This paper presents the results of a 5-year study using an UnCE and GCE device to measure the CCD of chloride-contaminated reinforced concrete specimens with various admixed chloride content in an outdoor exposure site.

2. Background

For a simple corroding system, Stern et al. [4] showed that the polarization curve for a few millivolts around the corrosion potential obeys a quasi-linear relationship. The slope of this relationship is called "polarization resistance" [4], as shown in Eq. (1):

$$R_p = (\Delta E/\Delta I)_{\Delta E \to 0} \quad (1)$$

This slope is related to the instantaneous corrosion current through the Stern–Geary equation as shown in Eq. (2):

$$I_{corr} = \frac{(\beta_a \beta_c)}{2.3 R_p (\beta_a + \beta_c)} = \frac{B}{R_p} \quad (2)$$

* Corresponding author. Tel.: +1-540-231-7408.
E-mail address: rweyers@vt.edu (R.E. Weyers).

0008-8846/03/$ – see front matter © 2003 Elsevier Science Ltd. All rigths reserved.
doi:10.1016/S0008-8846(03)00018-8

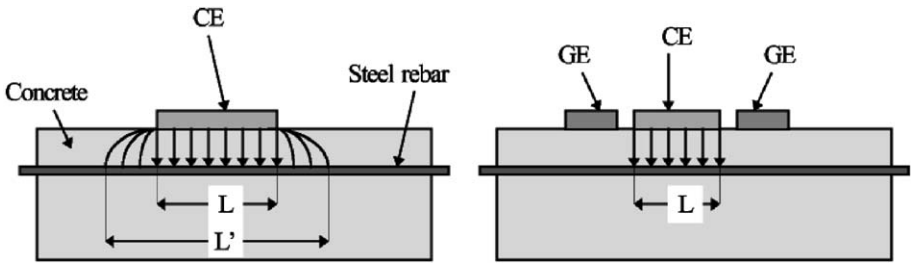

Fig. 1. A schematic diagram of UnCE and GCE device.

where β_a: the anodic Tafel slope; β_c: the cathodic Tafel slope; R_p: the polarization resistance; B: Stern–Geary constant.

The value of B is determined for a particular electrochemical cell and generally ranges from 13 to 52 mV depending on the system [5]. Based on the theories of polarization resistance to obtain evidence of corrosion activity, two devices which are currently used for measuring the CCD both in the laboratory and in the field are an UnCE [6] and a GCE device [7].

The UnCE device uses a counter-electrode (CE) to apply a cathodic current to the steel reinforcement, called the working electrode (WE). A third electrode, the reference electrode (RE), monitors the corresponding change in potential of the steel/concrete interface. The GCE device uses the same linear polarization technique as UnCE. The major difference between the devices is that the GCE device has a guard ring electrode which is used to confine the polarization current during the measurement process, see Fig. 1. The GCE device used in this study had a CE diameter of 80 mm with an estimated polarization bar length of 135 mm (halfway between the outer reference cells). Another significant difference is the polarization rate. The GCE polarization rate is device controlled based on the rate of corrosion, whereas the UnCE device is operator dependent within a set of guidelines. In addition, the devices use different Tafel slope values (B equals 40.7 and 26.0 mV for UnCE and GCE devices, respectively) in calculating the CCD. The result of these differences is approximately an order of magnitude difference in the measured CCD between the instruments. The general guidelines for interpreting the results of the UnCE [8] and GCE [9] as supplied by the instrument manufacturers are presented in Table 1.

Table 1
Guidance on interpretation of results of UnCE and GCE

i_{corr} ($\mu A/cm^2$)	GCE device	i_{corr} ($\mu A/cm^2$)	UnCE device
<0.1	passive	<0.2	no damage expected
0.1–0.5	low corrosion	0.2–1.1	damage possible 10–15 years
0.5–1.0	moderate	1.1–10.7	damage possible 2–10 years
>1.0	high corrosion	>10.7	damage possible <2 years

The linear polarization techniques have been widely used for measuring the CCD both in the laboratory and in the field [8,10,11]. The main difficulty involved in applying polarization resistance on-site is the definition of area over which the applied potential (or current) is acting or the polarized area. However, both devices use the area under CE as the nominal polarization area for calculating the CCD, 159 mm for the UnCE and 135 mm for the GCE.

Weight loss method (gravimetric technique) is a destructive method, which consists of weighing bar specimens before and after being introduced into the concrete. The detail test procedures for preparing, cleaning, and evaluating corrosion test specimens are described in ASTM G1 [12]. The average corrosion rate may be obtained as defined in Eq. (3):

$$\text{corrosion rate} = (K \times W)/(A \times T \times D) \quad (3)$$

where K is a constant, T is the exposure time, A is the surface area, W is the mass loss, and D is the density of the corroding metal. No instantaneous corrosion rates can be measured in this technique, but only the mean value over the period of test. The weight loss method is not without faults but is a precise method to quantify corrosion attack in laboratory experiments. Although this method is very time consuming and only applicable to the laboratory studies, it is a useful tool to check the accuracy of the electrochemical techniques that are able to measure the CCD quantitatively, such as the linear polarization and AC impedance techniques.

Table 2
Slab test matrix

Admixed chloride series (kg/m^3)	Cover depths for 16 mm bar at 203 mm spacing			Cover depth 50 mm, 16 mm bar, spacing 152 mm	Cover depth 50 mm, 19 mm bar, spacing 203 mm
	25	50	76		
0.0		2	2		
0.36		3	3		
0.71		3	3	3	3
1.42		3	3		
2.85		3	3		
5.69		3	3		
7.20	4				

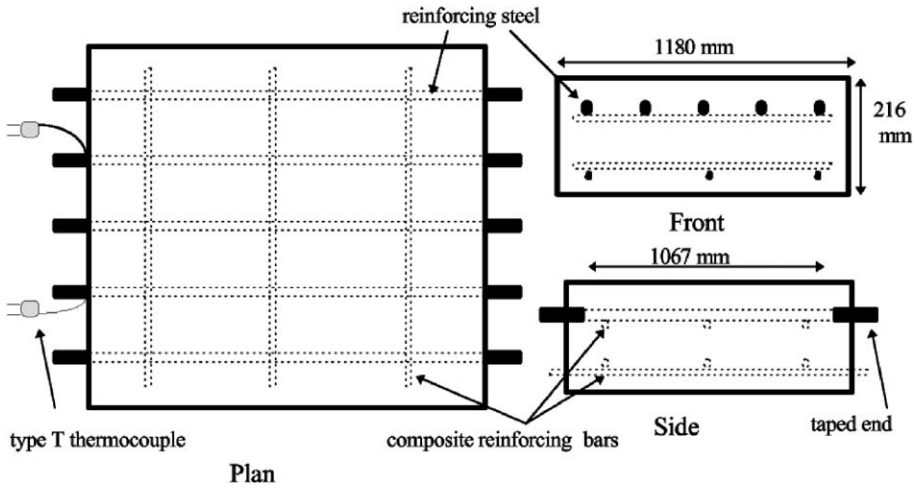

Fig. 2. A schematic diagram of the slab design.

In a 5-year study, the UnCE and GCE devices were used to measure the instantaneous CCD monthly on the different series of admixed chloride concrete specimens. Significant factors which influence the measured CCD were investigated. The weight loss method was also performed on the specimens immediately upon visual evidence of surface cracking. The results were then compared with that from the UnCE and GCE devices.

3. Experimental design

An experiment was designed to simulate typical concrete bridge deck construction conditions and investigate the influences of significant factors on the corrosion process in chloride-contaminated reinforced structures based on a sensitivity analysis of Bazant's model [13,14].

The experiment was designed with different CCD (different amount of chloride mixed into the concrete), two concrete cover depths and two reinforcing steel sizes and spacings. Forty outdoor exposure specimens were constructed with six series of admixed chloride contents, 0.0, 0.36, 0.71, 1.42, 2.85, and 5.69 kg/m^3, two concrete cover depths of 50 and 76 mm, two reinforcing steel diameters of 16 and 19 mm and two spacings of 152 and 203 mm. Four additional slabs were later cast with a higher admixed chloride, 7.2 kg/m^3, and thinner cover depth, 25 mm, which were estimated to crack within a short time period based on the observations and analyses over the 4 previous years. The number of test slabs within each test cell is presented in Table 2.

The simulated bridge deck slabs, concrete specimen of $1180 \times 1180 \times 216$ mm were constructed, with five electrical isolated reinforcing steel bars as shown in Fig. 2. The concrete mixture proportions are presented in Table 3, and the compressive strength tests results for each batch at 3, 7, and 28 days are summarized in Table 4. Type T thermocouples were placed at the depth of steel surface and used to determine the internal temperature of the steel/concrete interface at each measurement moment.

The UnCE and GCE devices were used to measure the CCD. Measurements were performed once a month, and concrete temperatures at the bar depth and ohmic resistances of the cover concrete were also recorded. The measurements were taken at midlength of each of the five electrically isolated bars for each slab. The bars remained electrically

Table 3
Mixture proportions

Chloride series (kg/m^3)	0.0	0.36	0.71	1.42	2.85	5.69	7.20
Cement (kg/m^3)	381	381	379	379	379	337	382
Water (kg/m^3)	173	160	159	155	167	162	172
W/C ratio	0.45	0.42	0.42	0.41	0.44	0.43	0.45
Coarse aggregate (kg/m^3)	1068	1068	1037	1079	1067	1078	1068
Fine aggregate (kg/m^3)	718	718	718	706	712	713	718
Daravair (g/m^3)	367	319	319	367	363	416	367
Salt, NaCl (kg/m^3)	0.0	0.6	1.2	2.4	4.8	9.6	12.0
Chloride (kg/m^3)	0.0	0.36	0.71	1.42	2.85	5.69	7.20
Slump (mm)	150	100	170	80	100	100	125
Unit weight (kg/m^3)	2232	2196	2148	2232	2232	2139	2197
Air content (%)	3.2	5.0	5.4	4.2	4.7	6.7	5.9

Table 4
Compressive strength of concrete

Admixed chloride series (kg/m^3)	0.0	0.36	0.71	1.43	2.85	5.69	7.20
Day 3 (MPa)	21.3	26.2	23.6	26.7	26.7	25.6	23.0
Day 7 (MPa)	25.8	30.8	28.8	32.0	30.8	28.7	27.4
Day 28 (MPa)	30.9	39.1	34.9	39.0	35.9	31.9	35.6

isolated during the measurement moment and throughout the 5-year study period. Metal loss measurements were performed in accordance with ASTM G1-90, Method C3.5 and compared with the measured corrosion values for specimens which cracked during the 5-year study period.

4. Results and discussions

The measured CCD from both the UnCE and GCE devices varied from time to time for the same admixed chloride series. Among the different series, the higher the admixed chloride content, the greater the measured CCD. Figs. 3–5 present the measured CCD, ohmic resistance of

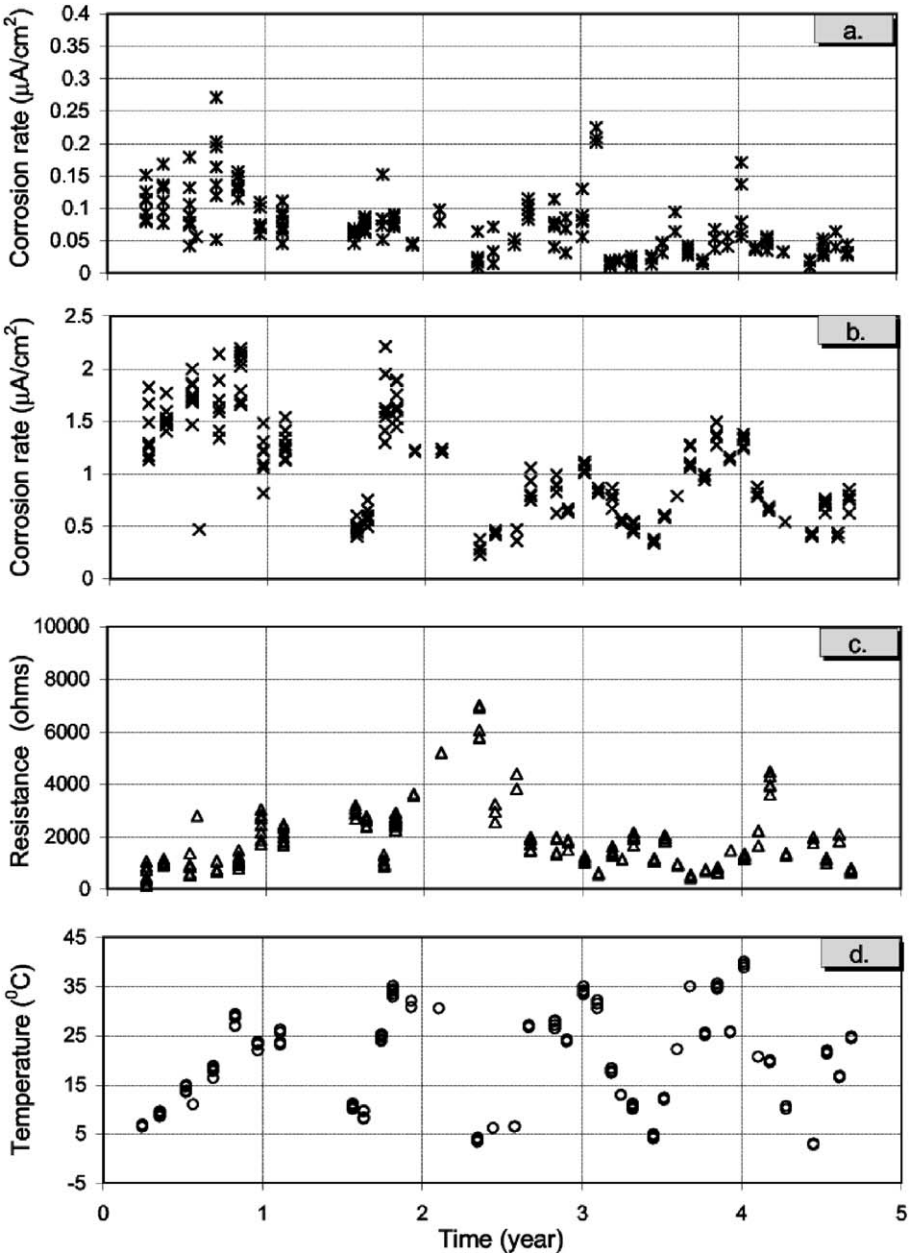

Fig. 3. Corrosion rate, concrete ohmic resistance, and temperature over corrosion time, 1.43 kg/m^3 admixed chloride, outdoor specimens, 51-mm cover depth. (a) Corrosion rate (GCE device) versus time; (b) corrosion rate (UnCE device) versus time; (c) concrete ohmic resistance versus time; (d) temperature at depth of reinforcement versus time.

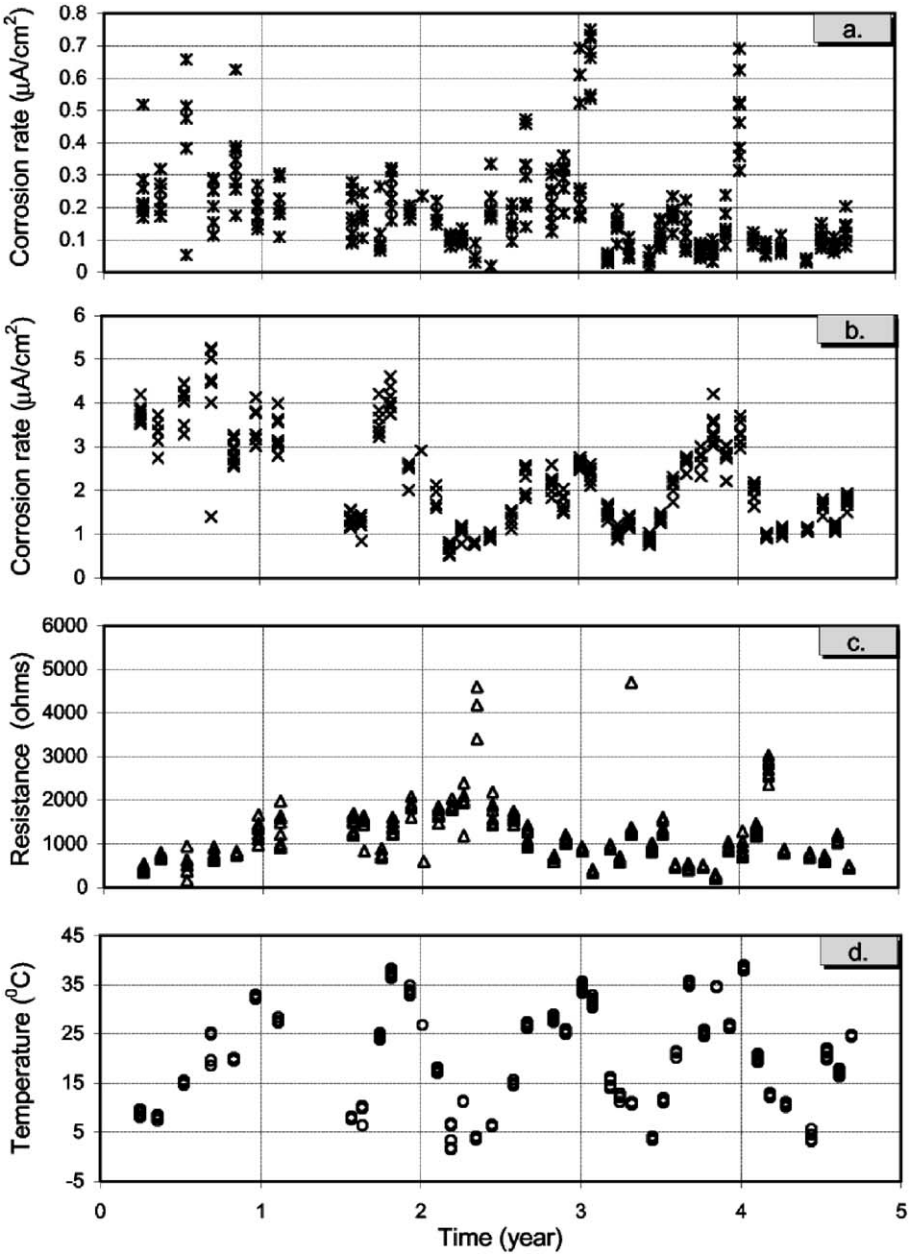

Fig. 4. Corrosion rate, concrete ohmic resistance, and temperature over corrosion time, 2.85 kg/m^3 admixed chloride, outdoor specimens, 51-mm cover depth. (a) corrosion rate (GCE device) versus time; (b) corrosion rate (UnCE device) versus time; (c) concrete ohmic resistance versus time; (d) temperature at depth of reinforcement versus time.

the cover concrete, temperature at depth of reinforcement over the measurement period for admixed chloride of 1.43, 2.85 and 5.69 kg/m^3, respectively. As shown, there is a significant difference, generally a factor of 10, between the results of the UnCE and GCE method. The results are generally in agreement with the results presented by other researchers [15]. In addition, the CCD are strongly dependent on concrete temperature, ohmic resistance, and chloride content. For UnCE measurements, a statistical model has been developed based on the obtained corrosion database (2927 measurements from seven series of chloride-contaminated specimens, 5 years outdoor exposure conditions) as presented in Eq. (4) [16]:

$$\ln i = 8.43 + 0.771 \ln Cl - 3006/T - 0.000116\, R_c + 2.24\, t^{-0.215} \quad (4)$$

where i is CCD (μA/cm^2), Cl is chloride content (acid soluble, kg/m^3), T is temperature (°K), R_c is ohmic resistance of cover concrete (ohms), and t is time (year). The above equation has a regression coefficient r of .95 and

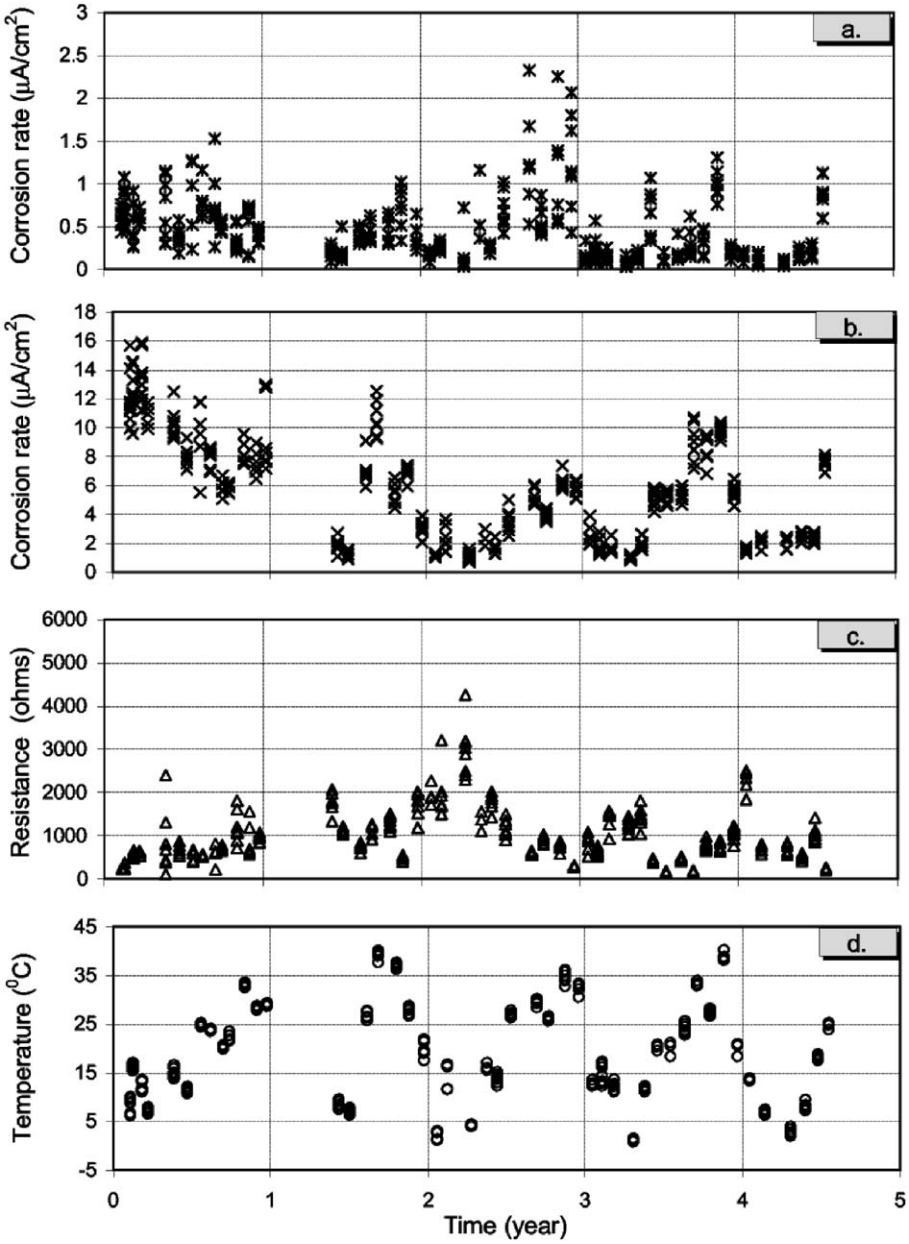

Fig. 5. Corrosion rate, concrete ohmic resistance, and temperature over corrosion time, 5.69 kg/m^3 admixed chloride, outdoor specimens, 51-mm cover depth. (a) corrosion rate (GCE device) versus time; (b) corrosion rate (UnCE device) versus time; (c) concrete ohmic resistance versus time; (d) temperature at depth of reinforcement versus time.

the root mean square error (RMSE) of 0.33. Fig. 6 presents the model predicted CCD and the measured values for the UnCE device. Due to the high variability (lack of precision) in the GCE measured CCD values within test corrosion cells [17], no such correlation was found for the measured CCD obtained from the GCE device.

Based on monthly CCD measurements by the UnCE and GCE devices, the mean corrosion CCD over time can be calculated by integration of the area under the time–CCD graphs. The results from the UnCE, GCE, and weight loss method are also summarized in Table 5. It appears that the results from the UnCE overestimate the CCD, whereas the results from the GCE underestimate the CCD based on weight loss measurements.

From the steel reinforcing sections taken from the cracked specimens, it was observed that the corrosion of steel was primarily pitting corrosion, not uniform corrosion, and most of the corrosion area was located on the upper half of the steel bar surface. It has been shown that the GCE is not able to properly confine the signal distribution below the CE under these conditions, when the corroding area is much smaller than the CE [18]. The polarization area under CE with GCE is smaller than that used for calculating the CCD for devices which use a

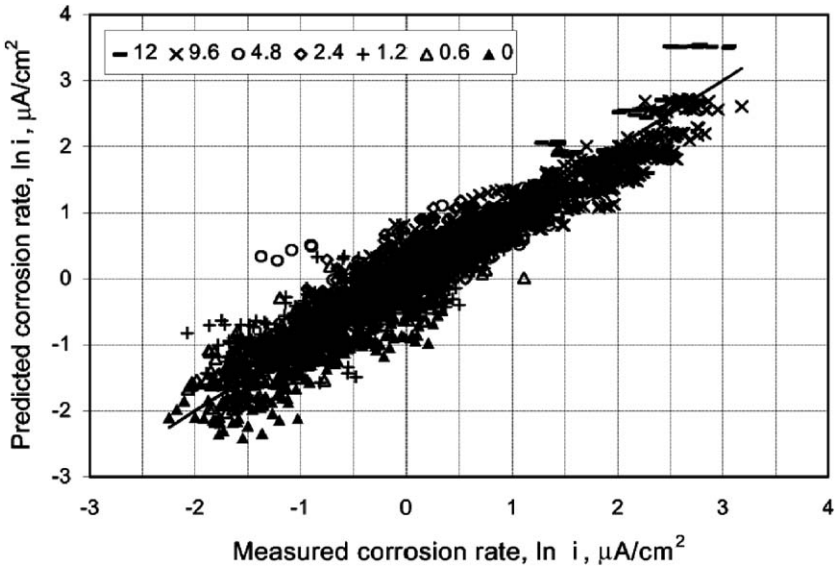

Fig. 6. Model-predicted corrosion rates versus measured corrosion rates (0.0, 0.6, 1.2, 2.4, 4.8, 9.6, and 12 series refer to 0.0, 0.36, 0.71, 1.43, 2.85, 5.69, and 7.20 kg/m^3 admixed chloride series, respectively).

guard ring as the GCE device, see in Fig. 7 [18]. This may cause a significant underestimation of CCD by the GCE device. Compared with weight loss measurements, the underestimation of the CCD by the GCE device is a factor of 4–6. Other analyses have shown that the polarization current using a guard ring is confined to the top half of the reinforcing steel [15]. Considering this and the observation that most of the corrosion was confined to the top half of the bar, an underestimate of a factor of 2 by the GCE device would result because the GCE device uses the bar diameter in calculating CCD, considering the above implications that the actual polarized bar length is smaller than that used to calculate the CCD and with only the top one-half of the bar being polarized. The actual polarization length may be about one-half to one-third of the bar length used in calculating the CCD. This overestimate of bar length polarization of device using guard rings is in agreement with previously presented analysis [18]. Of course, the above makes no correction for effects of concrete temperature and resistance and time after corrosion initiation over the measurement periods. Of course, no corrections for concrete temperature and resistance and time after corrosion initiation are possible for the GCE device because, as stated previously, no statistical significant relationship could be established for GCE device.

As shown in Table 5, the UnCE appears to have overestimated the CCD by a factor of 2.3–3.6 when compared to the weight loss measurements. A number of factors, as temperature and ohmic resistance of the concrete, affect the results of average CCD calculated from the UnCE measurements, see Eq. (4). The annual mean temperature in Blacksburg, VA is about 11 °C; while the measurements were taken on the outdoor specimens during the daylight hours when the temperatures at the depth of reinforcement varied between 2 and 43 °C. The mean temperature for the measurement times was definitely higher than that of annual mean temperature. This may cause an overestimation of the average CCD by the UnCE method. Using Eq. (4), adjusted average CCD were calculated for UnCE for an average temperature of 11 °C, concrete resistance and time after

Table 5
Corrosion current densities from different test methods

Test series	Exposure period (year)	Mean CCD (μA/cm^2)		
		Weight loss method	UnCE	GCE
18512.0 *	0.87	3.77	8.63	0.62
2859.6 *	1.84	2.34	8.19	0.50
3859.6 *	3.67	1.80	4.99	0.39

2859.6 series: 50 mm cover depth, 203 mm spacing, 16 mm diameter rebar, and 5.69 kg/m^3 admixed chloride; 3859.6 series: 76 mm cover depth, 203 mm spacing, 16 mm diameter rebar, and 5.69 kg/m^3 admixed chloride; 18512.0 series: 25 mm cover depth, 203 mm spacing, 16 mm diameter rebar, and 7.20 kg/m^3 admixed chloride.

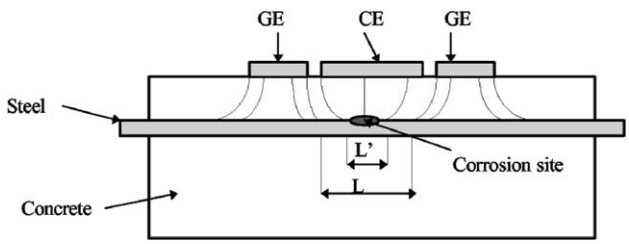

Fig. 7. A schematic diagram of signal distribution of GCE device in localized corrosion of steel in concrete.

corrosion initiation over the measurement periods. The results are presented in Table 6.

As shown in Table 6, the adjusted UnCE values are still about 1.5 times higher than that from the weight loss method. This may be related to the fact of a higher value of B (40.76 mV) used by the UnCE in calculating the CCD or a underestimation of the polarization area or both. The theoretical value of B has been shown to be 26 mV, the value used by the GCE device [18]. As seen in Fig. 1a, the actual length of signal distribution is much longer than that of the length of CE, while the polarization occurs mostly on the top half of the steel surface [15]. The overall actual polarization area may be still greater than the nominal polarization area used in calculation for the UnCE device.

As stated previously, the GCE device used in this study had a counter-electrode diameter of 80 mm and an estimated polarization bar length of 135 mm. Whereas present models have a counter-electrode diameter of 70 mm and a polarization length of 105 mm. The reduction in polarization length may improve the accuracy but questions still remain relative to the precision of the device. Of course, precision in this case is a combination of the device and the corrosion process. A considerable portion of the lack of precision may be attributed to the variability of the instantaneous CCD, that is, the corrosion process itself when measured over time, whereas devices, which do not use a guard ring, would measure a larger area than assumed and thus provide a more averaging CCD measurements and thus more precise but not accurate measurements.

With respect to accuracy of the measurements, weight loss measurements are not truly ground true measurements but also have limitations relative to accuracy of the measured phenomenon. However, more than accuracy, precision is needed in an engineering sense, which is the foundation in this study.

The authors have no differences in opinion of the relative interpretations of the GCE device presented in Table 1 of passive, low corrosion, moderate and high corrosion, but do present some concern in this study on the ability of the GCE device to be able to predict the time-to-cracking and spalling or calculating metal loss from a single or time series of measurements. The authors also have the same concerns about single UnCE measurements without the knowledge of the time of initiation of corrosion and other controlling CCD parameters as the increase in chloride content and the variation in concrete resistance and temperature over the time period from corrosion initiation to spalling of the cover concrete. Thus, the authors question the validity of the quantitative statements presented for the UnCE in Table 1.

In addition, it needs to be pointed out that the above observations are limited over the range of active CCDs of about 1.8–3.8 $\mu A/cm^2$ based on weight loss measurements from slabs which cracked during the 5-year measurement period. The devices provide the same rank ordering of CCDs, and thus, both devices may be used to qualitatively rank the severity of the CCD in concrete structures.

Table 6
Adjusted average corrosion current densities for the UnCE device and weight loss measurements

Series	Corrosion time (year)	W_{loss} ($\mu A/cm^2$)	UnCE ($\mu A/cm^2$)	Adjusted ($\mu A/cm^2$)	Adjusted/ W_{loss}
18512.0	0.87	3.77	8.63	5.96	1.58
2859.6	1.84	2.34	8.49	3.58	1.53
3859.6	3.67	1.80	4.99	2.79	1.55

5. Conclusions

1. For outdoor exposure condition, the measured instantaneous CCD from two commercial linear polarization devices were strongly dependent on environmental exposure conditions such as temperature, cover concrete ohmic resistance, chloride content, and time after initiation of corrosion and are able to qualitatively rank the instantaneous corrosion active in concrete structures.
2. The measured CCD at one time should be adjusted to an equivalent value corresponding with the service exposure conditions such as concrete temperature, resistance, and chloride content.
3. Comparing the measured CCD with the weight loss tests, the results from the GCE device underestimated the CCD by a factor of 4–6. The nominal polarization area used in the calculation being greater than the actual polarization area due to localized corrosion of steel in concrete and the inability to correct for environmental exposure conditions related to the lack of precision in the device measurements are the factors involved in this underestimation of CCD.
4. Comparing the measured CCD with the weight loss tests, the regression model (Eq. (4)) adjusted values for concrete temperature and resistance and time after corrosion initiation for the CCD for the UnCE device overestimated the CCD by a factor of about 1.55. The higher B constant value or a smaller nominal polarization area used in calculating the CCD or both may be the cause of this overestimation.

Acknowledgements

The research described herein was supported by the Strategic Highway Research Program (SHRP), the Center for Infrastructure Assessment and Management, College of Engineering, Virginia Polytechnic Institute and State University, and The Federal Highway Administration. The financial support of these organizations is gratefully acknowledged.

References

[1] K. Tuutti, Corrosion of Steel in Concrete, Swedish Cement and Concrete Research Institute, Stockholm, 1982.

[2] P.D. Cady, R.E. Weyers, Chloride penetration and the deterioration of concrete bridge decks, Cem. Concr. Aggr. 5 (2) (1983) 81–87.

[3] C. Andrade, C. Alonso, J.A. González, Approach to the calculation of the residual life in according to concrete reinforcements based on corrosion intensity value, 9th European Congress on Corrosion, 1989, Utrecht, The Netherlands, E & FN Spon, UK, 1989, pp. 18–22.

[4] M. Stern, A.L. Geary, Electrochemical polarization no. 1: theoretical analysis of the slope of polarization curve, J. Electrochem. Soc. 104 (1957) 56–63.

[5] C. Andrade, V. Castelo, C. Alonso, J.A. González, The determination of the CCD of steel embedded in concrete by the polarization resistance and AC impedance methods, ASTM Spec. Tech. Publ. 906 (1981) 43–63.

[6] Kenneth C. Clear, Test procedures, data analysis, and general information, K.C.C., 3-LP Package, 1990, Sterling, VA.

[7] Geocisa, Geotecnia Y Cimientos, Instructions manual for GCE corrosion-rate-meter, Geocisa, 1991, Madrid, Spain.

[8] Kenneth C. Clear, Measuring rate of corrosion of steel in field concrete structure, TRR (1211) (1990) 28–38.

[9] J.P. Broomfield, J. Rodriguez, L.M. Ortega, A.M. Garcia, Corrosion rate measurements in concrete bridges by means of the linear polarization technique implemented, A Field Device, Paper presented at ACI Fall Convention, 1993, Minneapolis, Minnesota, USA.

[10] S. Feliú, J.A. González, C. Andrade, V. Feliú, Determination of polarization resistance in reinforced concrete slabs, Corrosion 44 (10) (1988) 761–765.

[11] S. Feliú, J.A. González, S. Feliú Jr., C. Andrade, Confinement of electric signal for in situ measurement of polarization resistance in reinforced concrete, ACI Mater. J. 87 (1990) 457–460.

[12] Standard Practice for Preparing, Cleaning, and Evaluating Corrosion Test Specimens, ASTM G-1-90, Vol. 01.05, 1990, Philadelphia, PA.

[13] Z.P. Bazant, Physical model for steel corrosion in sea structures—applications, ASCE, J. Struct. Div. 105 (ST6) (1979, June) 1155–1166.

[14] J.E. Peterson, A Time to Cracking Model for Critically Contaminated Reinforced Concrete Structures, Masters of Science thesis, Virginia Polytechnic Institute and State University, December, 1993, Blacksburg, VA.

[15] J. Flis, et al., Condition evaluation of concrete bridges relative to reinforcement corrosion: vol. 2: Method for Measuring the CCD of Reinforcing Steel, SHRP-S/FR-92-104, Strategic Highway Research Program, National Research Council, 1992, Washington, DC.

[16] Y. Liu, Modeling the Time-to-Corrosion Cracking of the Cover Concrete in Chloride Contaminated Reinforced Concrete Structures, A dissertation presented to the Faculty of the Virginia Polytechnic Institute and State University, October, 1996, Blacksburg, VA.

[17] Y. Liu, R.E. Weyers, Time to cracking for chloride-induced corrosion in reinforced concrete, in: C.L. Page, B. Bamforth, J.W. Figg (Eds.), Corr. Reinf. Concr. Const., The Royal Society of Chemistry, Cambridge, UK, 1996, pp. 88–104.

[18] S.C. Kranc, A.A. Sagüés, Polarization current distribution and electrochemical impedance response of reinforced concrete when using the guard ring electrodes, Electrochim. Acta 38 (14) (1993) 2055–2061.